Acta Crystallographica Section D
Biological Crystallography
ISSN 1399-0047

Specific binding of gibberellic acid by Cytokinin-Specific Binding Proteins: a new aspect of plant hormone-binding proteins with the PR-10 fold

Milosz Ruszkowski,[a] Joanna Sliwiak,[a] Agnieszka Ciesielska,[a] Jakub Barciszewski,[a] Michal Sikorski[a] and Mariusz Jaskolski[a,b]*

[a]Center for Biocrystallographic Research, Institute of Bioorganic Chemistry, Polish Academy of Sciences, Poznan, Poland, and [b]Department of Crystallography, Faculty of Chemistry, A. Mickiewicz University, Poznan, Poland

Correspondence e-mail: mariuszj@amu.edu.pl

Received 6 April 2014
Accepted 8 May 2014

PDB references:
VrPhBP–GA3 complex, 4psb;
MtPhBP–GA3 complex, 4q0k

Pathogenesis-related proteins of class 10 (PR-10) are a family of plant proteins with the same fold characterized by a large hydrophobic cavity that allows them to bind various ligands, such as phytohormones. A subfamily with only ~20% sequence identity but with a conserved canonical PR-10 fold have previously been recognized as Cytokinin-Specific Binding Proteins (CSBPs), although structurally the binding mode of *trans*-zeatin (a cytokinin phytohormone) was found to be quite diversified. Here, it is shown that two CSBP orthologues from *Medicago truncatula* and *Vigna radiata* bind gibberellic acid (GA3), which is an entirely different phytohormone, in a conserved and highly specific manner. In both cases a single GA3 molecule is found in the internal cavity of the protein. The structural data derived from high-resolution crystal structures are corroborated by isothermal titration calorimetry (ITC), which reveals a much stronger interaction with GA3 than with *trans*-zeatin and pH dependence of the binding profile. As a conclusion, it is postulated that the CSBP subfamily of plant PR-10 proteins should be more properly linked with general phytohormone-binding properties and termed phytohormone-binding proteins (PhBP).

1. Introduction

Plant hormones (phytohormones) are chemical messengers that coordinate numerous cellular functions. This large group of molecules includes (but is not restricted to) ten main, chemically very diverse, classes: auxins, cytokinins, gibberellins, abscisic acid, brassinosteroids, ethylene, jasmonates, polypeptide hormones, salicylic acid and strigolactones (Santner *et al.*, 2009). Gibberellins, such as gibberellic acid (GA3; Fig. 1), are diterpenoid tetracyclic or pentacyclic growth regulators. They induce *inter alia* seed development and germination, organ elongation and flowering (Yamaguchi, 2008). Gibberellins were first discovered in *Gibberella fujikuroi*, a fungal pathogen of rice that causes extreme stem elongation, finally leading to plant collapse and death (Yabuta & Sumitki, 1938). Plants produce endogenous gibberellins and their cellular level is regulated not only *via* a negative-feedback loop but also by the concentration of auxins and ethylene (Fleet & Sun, 2005; Yamaguchi, 2008). The gibberellin receptor is known as gibberellin-insensitive dwarf1 protein (GID1), as loss-of-function mutations in the *gid1* gene cause dwarfism (Peng *et al.*, 1999), a feature desired in the cultivation of rice. Complexes of *Arabidopsis thaliana* GID1 with gibberellins have been investigated structurally by Murase *et al.* (2008) (PDB entries 2zsh and 2zsi). The GID1 receptor can bind DELLA proteins possessing a conserved Asp-Glu-Leu-Leu-Ala N-terminal sequence, which are

negative regulators of gibberellin response (Schwechheimer, 2008; Schwechheimer & Willige, 2009). In this mechanism, gibberellin binding by GID1 initiates GID1–DELLA complex formation. As a result, the DELLA proteins can no longer function as transcription repressors of gibberellin-dependent genes and are instead ubiquitinated and targeted for degradation.

On the other hand, cytokinins, such as *trans*-zeatin (ZEA), which are adenine derivatives, stimulate cell division (cytokinesis) and differentiation in various developmental processes. Cytokinins take part, for example, in apical dominance, axillary bud growth, leaf senescence, flowering and response to pathogens. In legume plants such as *Medicago truncatula* and *Vigna radiata* cytokinins also control root nodulation during symbiosis with nitrogen-fixing soil bacteria.

Pathogenesis-related proteins of class 10 (PR-10) are small (up to 19 kDa), usually monomeric, slightly acidic, cytosolic plant-specific proteins (Fernandes *et al.*, 2013). The name pathogenesis-related is quite misleading as it is now well established that PR-10 proteins are expressed not only during pathogenesis (van Loon *et al.*, 2006). Despite many years of study, however, the exact biological function of PR-10 proteins remains unknown. In contrast, the structural conservation of PR-10 proteins is well established and forms the basis of the canonical PR-10 fold. The fold consists of a curved seven-stranded antiparallel β-sheet crossed by a long C-terminal helix (α3), supported at its carboxy end by a V-shaped motif of two shorter helices (α1 and α2). The most prominent feature of this fold is a large hydrophobic cavity formed between helix α3 and the β-sheet (Chwastyk *et al.*, 2014) that is evidently the binding site for PR-10 ligands. However, even the nature of the physiological binding partners of the PR-10 proteins remains obscure. A group of promising candidates are cytokinins, but while several crystallographic studies did confirm the potential of PR-10 proteins to bind cytokinins, the complexes also revealed a perplexing diversity of ligand interactions and binding modes, and even a highly variable stoichiometry (Pasternak *et al.*, 2006; Fernandes *et al.*, 2008, 2009; Kofler *et al.*, 2012). Only recently, a PR-10 protein involved in root nodulation, nodulin MtN13, was found to form highly specific and structurally conserved complexes with different cytokinins, although the complexes turned out to have an unusual dimeric structure (Ruszkowski *et al.*, 2013).

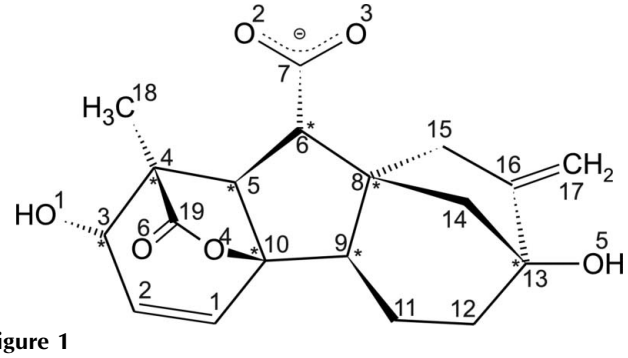

Figure 1
Chemical structure of gibberellic acid (GA3) with atom numbering. Asterisks indicate chiral C atoms.

Historically, a subclass of proteins with a conserved PR-10 fold, despite very low sequence identity (~20%) to other PR-10 proteins, was identified by Fujimoto *et al.* (1998) as strong cytokinin binders. The reported exceedingly high (nanomolar) cytokinin affinity was later corrected (Pasternak *et al.*, 2006) by five orders of magnitude (high micromolar), but the term Cytokinin-Specific Binding Proteins (CSBPs) has been well established in the literature. CSBP proteins are only found in legume plants and are expressed at such low levels that Fujimoto *et al.* (1998) had to use 95 kg of etiolated mung bean (*V. radiata*) seedlings for the detection and N-terminal sequencing of VrCSBP. The crystal structure of VrCSBP in complex with ZEA (Pasternak *et al.*, 2006) revealed that neither the binding mode nor the stoichiometry were conserved in the four protein molecules found in the asymmetric unit. This led to the assumption that cytokinins might be in fact not the preferred physiological ligands of the CSBP proteins. In an independent study, Zawadzki *et al.* (2010) reported that VrCSBP also interacted with gibberellins. The latter results were obtained in indirect experiments using fluorescence correlation spectroscopy to monitor the displacement of *trans*-zeatin (labelled with a large chromophore moiety) by gibberellic acid.

In the present work, we have focused on the question of whether two CSBP proteins from *M. truncatula*, which is a model legume plant, and from *V. radiata* could be demonstrated to interact with gibberellins in direct experiments using crystallography and isothermal titration calorimetry (ITC). The question has been answered positively, as our crystallographic results unambiguously show that both proteins bind GA3 with 1:1 stoichiometry and that the binding mode is strictly conserved in the two complexes. The crystallographic results were supported by ITC measurements, which showed that the proteins bind GA3 much more strongly than *trans*-zeatin and that the binding is pH-dependent. From these observations, we conclude that the proteins classified so far as CSBPs should be more properly recognized as more general phytohormone binders. Consequently, we propose to replace the term CSBP with PhBP (phytohormone-binding proteins), and we use the latter acronym throughout the remaining part of this article.

2. Materials and methods

2.1. Cloning, overexpression and purification of PhBP proteins

The MtPhBP DNA coding sequence was amplified by polymerase chain reaction (PCR) using *M. truncatula* (ecotype J5) cDNA as template. The reaction product was cloned into the pET-TOPO-151D vector (Invitrogen) and the correctness of the insert was confirmed by sequencing. The vector introduces an N-terminal His_6 tag followed by the cleavage site for TEV (*Tobacco etch virus*) protease and a hexapeptide linker (GIDPFT) that precede the genuine protein sequence. Overexpression was carried out in *Escherichia coli* BL21 (DE3) cells. The cells were disrupted by sonication using bursts of

total duration 4 min with appropriate intervals for cooling. Cell debris was removed by centrifugation at 15 000 rev min^{-1} for 30 min at 4°C. The supernatant was applied onto a column packed with 6 ml HisTrap HP resin (GE Healthcare). After binding, the column was washed four times with 30 ml binding buffer (50 m*M* Tris–HCl pH 8.0, 500 m*M* NaCl, 20 m*M* imidazole) and the purified protein was eluted with 15 ml elution buffer (50 m*M* Tris–HCl pH 8.0, 500 m*M* NaCl, 200 m*M* imidazole). The His_6 tag was cleaved with TEV protease and the excess imidazole was removed by dialysis (overnight at 4°C) simultaneously. The solution was mixed in a column with HisTrap HP resin to remove the His_6-tag debris and the His_6-tagged TEV protease. The flowthrough was collected, concentrated to 4 ml and applied onto a HiLoad Superdex 200 16/60 column (GE Healthcare) equilibrated with 5 m*M* sodium citrate pH 6.3. The sample was concentrated to 10 mg ml^{-1} as determined by the method of Bradford (1976) and used for crystallization experiments. VrPhBP was produced and purified as described previously (Bujacz *et al.*, 2003).

2.2. Crystallization and data collection

Protein solutions at 10 mg ml^{-1} (MtPhBP) and 13 mg ml^{-1} (VrPhBP) concentration were incubated overnight with GA3 (Sigma–Aldrich, catalogue No. 63492) added as a 10 mg ml^{-1} solution in 10% aqueous ethanol. A threefold molar excess of GA3 was used in both crystallization experiments. Following overnight incubation, the protein–ligand mixtures were centrifuged at 14 000 rev min^{-1} for 5 min at room temperature to remove the precipitated protein. The crystallizations were carried out in hanging drops using the vapour-diffusion method. The crystallization reservoir for MtPhBP was composed of 0.1 *M* ADA buffer pH 6.5, 1.0 *M* ammonium sulfate and the drops were composed of 1 µl protein–ligand solution and 1 µl reservoir solution. In the case of VrPhBP, the crystals were grown using a reservoir solution consisting of 0.1 *M* MMT buffer pH 4.0, 25% PEG 1500 and the crystallization drops were composed of 4 µl protein–ligand solution and 2 µl reservoir solution. The crystals of the complexes appeared after ten months (MtPhBP) or one week (VrPhBP) at 19°C. The reservoir solutions supplemented with 30 or 20% glycerol were used for cryoprotection of the crystals of the MtPhBP or VrPhBP complexes, respectively. The crystals were vitrified in liquid nitrogen and stored for synchrotron-radiation data collection. The diffraction data were processed and scaled using *XDS* (Kabsch, 2010) with data statistics as summarized in Table 1.

2.3. Determination and refinement of the crystal structures

The crystal structures of both complexes were solved by molecular replacement using *Phaser* (McCoy *et al.*, 2007). Protein chain *A* of VrPhBP retrieved from its complex with ZEA (PDB entry 2flh; Pasternak *et al.*, 2006) served as the search probe. In the case of MtPhBP, automatic model building was carried out with the online version of *ARP*/*wARP* (Langer *et al.*, 2008). *Coot* (Emsley *et al.*, 2010) was used for manual fitting in electron-density maps between rounds of model refinement in *phenix.refine* (Adams *et al.*, 2010; Afonine *et al.*, 2012). Anisotropic atomic displacement parameters were refined for all (non-H) atoms. Riding H atoms for the protein molecules were included in F_c calculations for both complexes. Geometrical restraints for the GA3 ligand were generated in *phenix.elbow* (Moriarty *et al.*, 2009) using target values from entry BUWZAU (Kutschabsky & Gunter, 1983) in the Cambridge Structural Database (CSD; Allen, 2002). The final models were validated with *MolProbity* (Chen *et al.*, 2010). The refinement statistics are listed in Table 1.

Table 1
Data-collection and refinement statistics.

Values in parentheses are for the highest resolution shell.

GA3 complex with	MtPhBP	VrPhBP
Data collection		
Radiation source	BESSY, Berlin	PETRA III, DESY Hamburg
Beamline	14.2	P14
Wavelength (Å)	0.918000	0.975507
Temperature (K)	100	100
Space group	$P6_5$	$C2$
Unit-cell parameters (Å, °)	$a = b = 55.8$, $c = 100.0$	$a = 33.4$, $b = 54.3$, $c = 71.1$, $\beta = 98.7$
Resolution (Å)	34.74–1.34 (1.44–1.34)	35.06–1.42 (1.46–1.42)
Reflections (total/unique)	415195/38199	119545/24350
Completeness (%)	97.8 (88.3)	99.5 (99.3)
Multiplicity	10.9 (5.6)	4.9 (4.7)
R_{merge}† (%)	4.3 (87.2)	7.9 (52.0)
$\langle I/\sigma(I)\rangle$	30.64 (1.91)	9.20 (1.98)
Refinement		
Unique reflections (work + test)	38196	24350
Test reflections	1000	1023
Matthews coefficient (Å^3 Da^{-1})	2.58	1.87
Solvent volume (%)	52.4	34.4
No. of atoms (non-H)		
Protein	1265	1268
GA3/glycerol	25/30	25/0
Solvent	197	143
R_{work}/R_{free} (%)	12.4/15.7	15.4/20.4
R.m.s.d. from ideal geometry		
Bond lengths (Å)	0.019	0.019
Bond angles (°)	1.6	1.9
Ramachandran statistics (%)		
Favoured	98.7	98.7
Allowed	1.3	1.3
PDB code	4q0k	4psb

† $R_{merge} = \sum_{hkl}\sum_i |I_i(hkl) - \langle I(hkl)\rangle| / \sum_{hkl}\sum_i I_i(hkl)$, where $I_i(hkl)$ is the intensity of observation i of reflection hkl.

2.4. Isothermal titration calorimetry

All ITC experiments were carried out at 20°C using a MicroCal iTC200 calorimeter (GE Healthcare). Both proteins, MtCSBP and VrCSBP, were dialyzed against either 150 m*M* NaCl, 25 m*M* MES pH 5.5 or 150 m*M* NaCl, 25 m*M* HEPES pH 7.4 buffer before titration. GA3 and ZEA were dissolved in the dialysis buffers to concentrations of 0.9 and 1.5 m*M*, respectively. The protein concentration in the sample cell was determined by the Bradford assay (Bradford, 1976) and was adjusted each time to within the range 80–100 µ*M*.

Phytohormone concentrations were determined gravimetrically by weighing a sample at least 100-fold heavier than the balance sensitivity of 0.1 mg. The ligands (GA3 or ZEA) were injected in 1.5 µl aliquots until saturation was observed. Raw ITC data were analyzed with the *Origin* 7.0 software (OriginLab) to obtain the following parameters: stoichiometry (N), dissociation constant (K_d) and the changes in the enthalpy (ΔH) and entropy (ΔS) during the complexation reaction. For the hyperbolic curves (for which determination of N is impossible) which were obtained from titrations of VrPhBP with ZEA, a sequential binding sites model for two binding sites was imposed on the basis of the crystal structure of the VrCSBP–ZEA complex (Pasternak *et al.*, 2006). For sigmoidal curves obtained from titrations with GA3, a one set of sites model was fitted and N (stoichiometry) was determined from the titration experiment. A competitive binding assay (GA3 *versus* ZEA) performed at pH 5.5 was designed in the same way as the simple titration with GA3, with the additional presence of ZEA at 433 µM concentration in the sample cell. All ITC experiments were performed in triplicate.

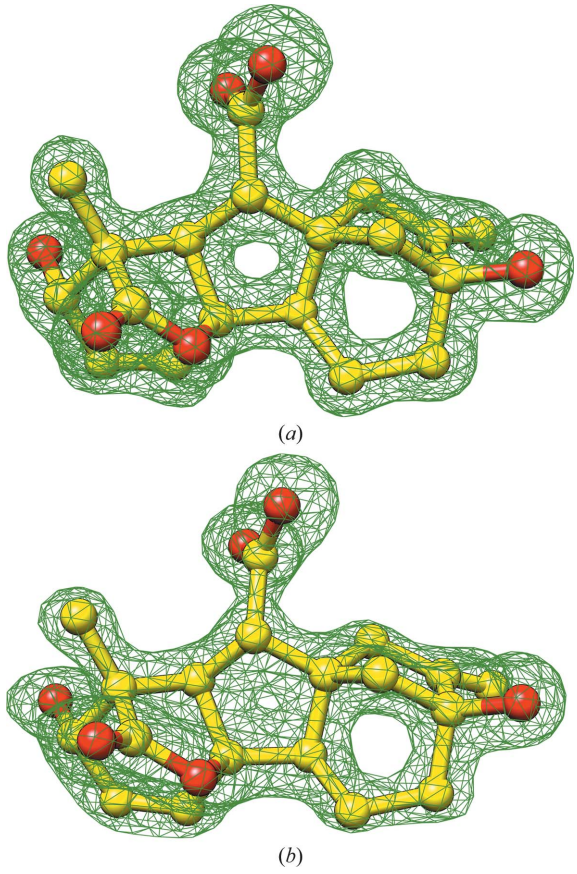

Figure 2
Electron-density maps of gibberellic acid (ball-and-stick representation) bound in the presented complexes with MtPhBP (*a*) and VrPhBP (*b*). OMIT $F_o - F_c$ electron-density maps (green mesh) are contoured at the 4σ level.

2.5. Other software used

Assignment of secondary-structure elements was based on the *DSSP* algorithm (Kabsch & Sander, 1983). Potential quaternary structures were analyzed with *PISA* (Krissinel & Henrick, 2007). Surfaces of protein internal cavities were calculated with *SURFNET* (Laskowski, 1995). *UCSF Chimera* (Pettersen *et al.*, 2004) was used for structural alignments and for the preparation of molecular figures. *ClustalW* (Larkin *et al.*, 2007) was used for sequence alignment.

3. Results and discussion

3.1. Overall structural properties of the PhBP–GA3 complexes

Both MtPhBP and VrPhBP are monomeric in solution, as they elute as monomers in size-exclusion chromatography (not shown). Likewise, no stable quaternary structure could be predicted from crystal packing by *PISA* (Krissinel & Henrick, 2007). The two complexes crystallize in different space groups, namely $P6_5$ (MtPhBP) and $C2$ (VrPhBP). In both crystals there is one copy of a 1:1 PhBP complex with GA3 in the asymmetric unit. The different crystal packing is reflected in a different Matthews volume (Matthews, 1968) and in different solvent contents: 52.4 and 34.4% for MtPhBP and VrPhBP, respectively. Despite the different levels of hydration, crystals of both complexes diffracted X-rays to very high angles, which allowed refinement of the crystal structures at the very high resolutions of 1.34 and 1.42 Å, respectively. Owing to the high data resolution, the atomic displacement parameters could be refined anisotropically. The final electron-density maps are of excellent quality in both cases. The entire protein chains starting with Met1 could be modelled with confidence, except for two residues (–GA) at the C-terminus in the case of MtPhBP and three (–GSA) in the case of VrPhBP, which were disordered and were thus omitted from the models. The GA3 ligand in both complexes had superb definition in $F_o - F_c$ electron-density maps phased using the protein atoms only, and could be modelled without any ambiguity (Fig. 2). Five glycerol molecules from the cryoprotectant solution could be traced in the electron-density maps of the MtPhBP complex. Two of those glycerol molecules are found near the entrance to the internal cavity. One glycerol molecule is hydrogen-bonded to Ser23 and one to Asp47. Another

Figure 3
Sequence alignment of MtPhBP and VrPhBP, with annotation of secondary-structure elements as assigned by *DSSP* (Kabsch & Sander, 1983). Loops are labelled L1–L9. Black and grey shadings indicate identical and similar residues, respectively.

glycerol molecule is close to the N-terminus, interacting *via* a water-mediated hydrogen bond with Glu4.

The two protein molecules in this study, MtPhBP and VrPhBP, share 74% sequence identity and 86% similarity. Their sequence alignment with secondary-structure assignment is shown in Fig. 3. Both proteins have the canonical PR-10 fold (Fig. 4*a*), with a seven-stranded antiparallel β-sheet wrapped around the C-terminal helix α3. The consecutive β-strands are connected by β-hairpins and loops, except for the β1–β2 crossover, which is formed by helices α1 and α2 that link the edges of the β-sheet. The β-sheet has a highly curved shape induced by eight β-bulges. Overall, the fold of the proteins resembles a right-handed baseball glove, where the odd-numbered loops (L3, L5, L7 and L9) form the 'fingers'. The two short helices α1 and α2 create a V-shaped support for the C-terminal part of the long α3 helix, which forms the 'thumb' of the glove. A single α-helical turn within loop L7, formed by four residues (Gly90–Asn93 in MtPhBP and Gly89–Ser92 in VrPhBP), is disregarded in the following discussion to maintain consistency of secondary-structure numbering with other PR-10 proteins. In the topology of PR-10 proteins, the internal cavity, which is often a ligand-docking site, is formed between the β-sheet and the α3 helix. This is also the case for the present PhBP complexes, where the gibberellic acid molecule is located inside this internal cavity in both structures (Figs. 4*b* and 4*c*). The structural details of GA3 docking are discussed in the next section.

The backbones of MtPhBP and VrPhBP are quite similar, as illustrated by the r.m.s. (root-mean-square) deviation between their C^{α} positions of 0.69 Å. Most of the few differences of significance are observed within loops, in particular in loop L9, which is the point of entry for helix α3 (Fig. 4*a*). Loop L9 is one of the most variable structural elements of the PhBP subfamily of PR-10 proteins. In particular, in the VrPhBP–ZEA complex (Pasternak *et al.*, 2006) loop L9 of chain *A* could not be traced in the electron-density maps (residues 123–129) or was involved in Na^{+} coordination in chains *B* and *C*, while in chain *D* it was visible but metal-free. In contrast, the so-called glycine-rich loop L4 with the sequence motif $_{44}$(IV)EG(ND)GG(PV)GT$_{52}$ is sequentially conserved and structurally rigid as in all other PR-10 structures.

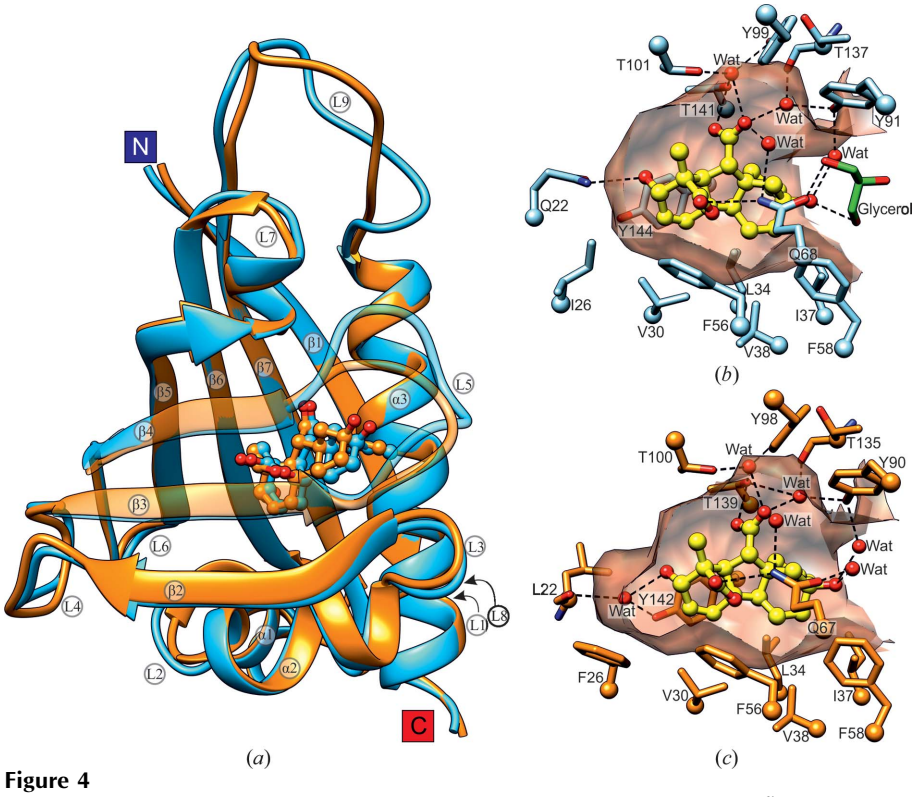

Figure 4
Gibberellic acid binding by PhBP proteins. (*a*) Overall fold of the PhBP proteins (C^{α} superposition) in their GA3 complexes, shown as a cartoon model with MtPhBP in blue and VrPhBP in orange. Secondary-structure elements are numbered according to the PR-10 canon. The N- and C-termini are also marked. Strands β3 and β4 and loop L5 are semitransparent to visualize the phytohormone molecule in the internal binding cavity. Note that the GA3 molecules (ball-and-stick representation) are in the same position and orientation in both complexes. Close-up view of the GA3 binding site of MtPhBP (*b*) and VrPhBP (*c*). Hydrogen bonds are shown as dashed lines. The entrance to the internal cavity is on the right side of each panel. Protein surfaces that form the walls of the cavity have been clipped to show a maximum vista and are presented in semitransparent red. C^{α} atoms are highlighted as balls. A glycerol molecule (*b*, green) originates from the cryoprotectant buffer. The backbone C, O and N atoms of the protein chains have been omitted for clarity unless they take part in binding interactions, as is the case for Thr137 in MtPhBP and Leu22 and Thr135 in the VrPhBP complex.

3.2. Structural details of gibberellic acid binding

The GA3 molecules bound to MtPhBP and VrPhBP are found deep in the internal cavities of the proteins. The cavity is the most fascinating structural element of all PR-10 proteins, as it gives rise to an essentially hollow protein core without degrading the mechanical properties of the molecule (Chwastyk *et al.*, 2014). In the present structures several hydrophobic residues shape the walls of the cavities (Figs. 4*b* and 4*c*). These nonpolar residues are perfect partners for interactions with the hydrophobic fragments of the GA3 molecule. The hydrophobic interaction surface of the protein cavity is formed by the side chains of Ile26/Phe26 (MtPhBP/VrPhBP), Val30, Leu34, Ile37, Val38, Phe56 and Phe58. There is also a stabilizing stacking interaction between the π-electrons of the double C1=C2 bond of GA3 and a parallel aromatic ring of Tyr144 (MtPhBP) or Tyr142 (VrPhBP), located within a distance of ~4 Å. The conservation of these hydrophobic and Tyr residues strongly suggests that they are required for specific interactions with a ligand, and hence that the complexes observed in our crystals are in all likelihood of biological significance.

Table 2
Hydrogen bonds between GA3 and MtPhBP/VrPhBP, with donor–acceptor distances (Å) in parentheses.

In the case of water-mediated or glycerol-mediated hydrogen bonds only the immediate interactions with the solvent molecules are listed and the protein residues serving as the ultimate docking sites are discussed in the text.

Atom	MtPhBP	VrPhBP
O1	Gln22 N^{ε} (3.2)	Wat1† (2.7)
O2	Thr141 O^{γ} (2.7)	Thr139 O^{γ} (2.7)
O3	Wat1 (2.7)	Wat2 (2.6)
	Wat2 (2.7)	Wat3 (2.7)
	Wat3 (2.7)	Wat4 (2.8)
O5	Glycerol (3.1)	Wat5 (2.6)
	Wat4 (2.7)	Wat6 (3.1)
O6	Gln68 N^{ε} (3.1)	Gln67 N^{ε} (3.2)

† Labels of water molecules in the table are assigned in each complex sequentially and do not correspond to the numbers in the PDB entries.

Table 3
Thermodynamic characterization of the interactions of MtPhBP and VrPhBP with GA3 (gibberellic acid) and ZEA (*trans*-zeatin).

The stoichiometry N, the dissociation constant K_d (μM), the change in enthalpy ΔH (cal mol^{-1}) and the change in entropy ΔS (cal mol^{-1} K^{-1}) were determined by ITC titrations at pH 5.5 and 7.4.

Protein	MtPhBP		VrPhBP	
pH	7.4	5.5	7.4	5.5
GA3				
N	†	1.14 ± 0.01	1.17 ± 0.01	1.09 ± 0.01
K_d		13.4 ± 0.5	23 ± 1	6.1 ± 0.2
ΔH		−3727 ± 35	−8054 ± 120	−9039 ± 63
ΔS		9.6	−6.3	−7.0
ZEA				
K_{d1}	‡	‡	76 ± 1	181 ± 25
ΔH_1			−5186 ± 59	−6645 ± 493
ΔS_1			1.16	−5.6
K_{d2}			67 ± 1	94 ± 9
ΔH_2			1903 ± 71	4348 ± 573
ΔS_2			25.6	33.2

† No heat effect. ‡ A very small enthalpy change (ΔH < 800 cal mol^{-1}) and a high noise-to-signal ratio precluded reliable estimation of the derived parameters.

In addition to the hydrophobic interactions, several hydrogen bonds are formed between the gibberellic acid and the protein. The GA3 molecule has six O atoms of different chemical character. Two of them belong to the carboxyl group, two are in hydroxyl groups and two other form the lactone moiety. In the present complexes, all of the O atoms of GA3 except for the endocyclic O4 atom interact with the protein *via* hydrogen bonds (Figs. 4*b* and 4*c*, Table 2). Three (Gln22, Gln68 and Thr141) or two (Gln67 and Thr139) residues form direct hydrogen bonds to GA3 in the MtPhBP or VrPhBP complexes, respectively. In addition, there are several solvent-mediated hydrogen bonds that ultimately link the GA3 molecules to Gln68, Tyr91, Tyr99, Thr101 and Thr137 in MtPhBP or to Leu22, Gln67, Tyr90, Tyr98, Thr100, Thr135 and Tyr142 in VrPhBP.

In contrast to the extensive similarities of the interior of the GA3 binding sites, there are significant differences in the surface areas adjacent to the entrance leading to the cavity (Fig. 5). In MtPhBP this portion of the protein surface is only slightly charged, with only three residues, Lys131, Lys136 and Glu139, contributing to the electrostatic potential of this side of the protein surface. Moreover, the positive charge of Lys136 is compensated by the negative charge of the Glu139 side chain. The situation is very different in the VrPhBP protein, where nine charged residues (Glu61, Glu127, Glu128, Lys129, Lys134, Gln137, Arg144, Arg145 and Arg148) surround the entrance to the internal cavity. Moreover, these highly polar residues are segregated sidewise, meaning that the negative charge is concentrated on one side of the cavity (left in the view presented in Fig. 5*b*), while the positive charge is concentrated on the opposite (right) side. The difference in the surface-charge distribution in the vicinity of the entrance to the cavity explains why, according to the ITC experiments (see below), VrPhBP is capable of binding GA3 (as an anion) at pH 7.4 whereas MtPhBP is not.

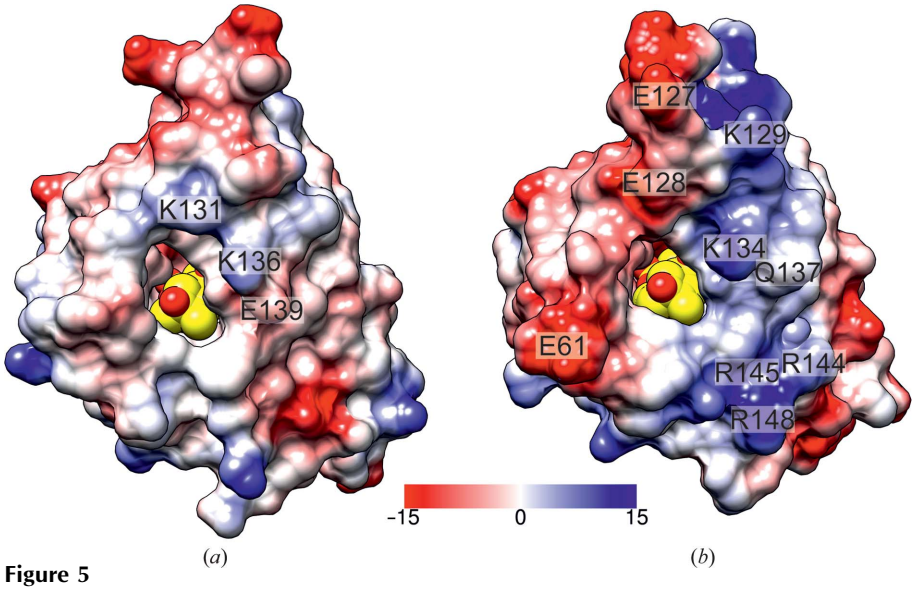

Figure 5
Electrostatic potential surface around the entrance to the internal cavity. MtPhBP (*a*) and VrPhBP (*b*) are viewed in the same orientation to show the GA3 molecule (yellow C-atom spheres) bound inside the cavity. The electrostatic potential is colour-coded according to the scale bar, which is calibrated in kT e^{-1} units.

The binding mode of gibberellic acid in PhBP complexes is quite different from that reported for the gibberellin receptor GID1 (Murase *et al.*, 2008). There are, however, three similar aspects between the PhBP and GID1 complexes that need to be addressed. Firstly, in both cases the GA3 molecule is oriented in the ligand-binding site in such a way that the lactone moiety is buried deeply in the cavity, whereas the C13 OH group points towards solvent/cytoplasm. Secondly, the docking of GA3 occurs *via* only three direct hydrogen bonds, whereas the remaining

heteroatoms of GA3 interact with the protein through water-mediated contacts. Thirdly, the endocyclic O4 atom of the lactone ring is the only GA3 O atom that does not form any hydrogen bonds.

It is noted that a GA3 restraint library based on the CSD structure BUWZAU corresponds to the acidic (protonated) form of the carboxylic group of the ligand. Because there is no crystal structure of GA3 in the anionic form, this library was used with both carboxylate C—O bond lengths set to 1.254 Å. In the crystal structure of MtPhBP, which was formed at pH 6.5, the ligand is expected to be in the anionic state because the pK_a value of gibberellic acid is 4.0 (Tomlin, 1997). In the structure of the VrPhBP complex formed at pH 4.0, one could theoretically expect a half-protonated carboxylic group of GA3. However, since refinement at even 1.42 Å resolution does not allow carboxylic/carboxylate groups to be unambiguously distinguished and since the pattern of hydrogen bonds at the GA3 molecule is not univocal, the ligand has been treated as an anion in this paper.

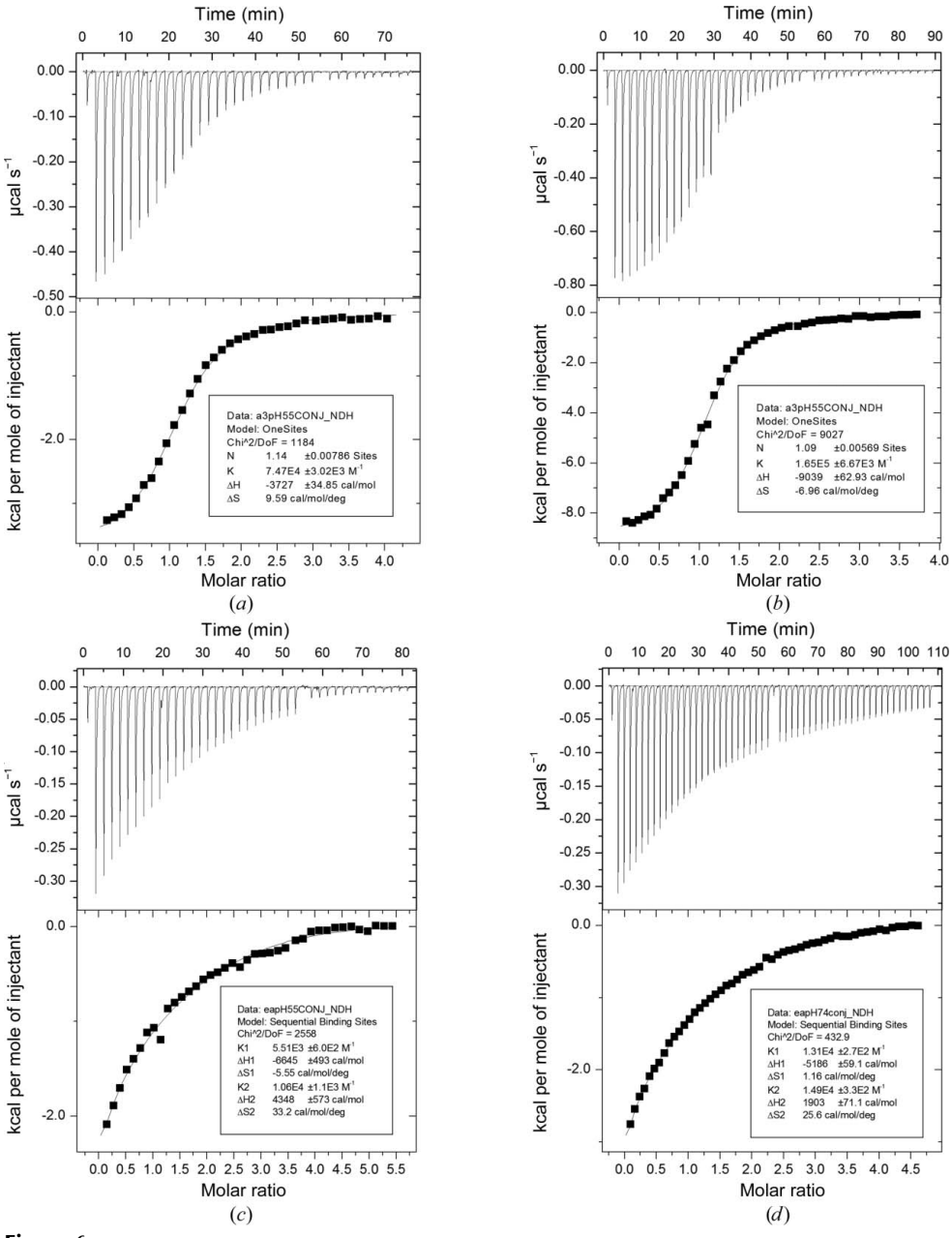

Figure 6
Calorimetric titrations of PhBP proteins with GA3 (*a*, *b*) and ZEA (*c*, *d*). The top plot of each panel shows the raw heat data obtained from ∼40 consecutive injections of GA3 or ZEA into the sample cell (200 µl) containing MtPhBP (*a*) or VrPhBP (*b*, *c*, *d*). The experimental conditions were as follows: (*a*) 105 µ*M* MtPhBP, 1.5 m*M* GA3, pH 5.5, (*b*) 80 µ*M* VrPhBP, 0.9 m*M* GA3, pH 5.5, (*c*) 93 µ*M* VrPhBP, 1.5 m*M* ZEA, pH 5.5 and (*d*) 100 µ*M* VrPhBP, 1 m*M* ZEA, pH 7.4. The titrations were performed at 290.15 K in a buffer composed of (*a*, *b*, *c*) 25 m*M* MES pH 5.5 or (*d*) 25 m*M* HEPES pH 7.4 supplemented with 150 m*M* NaCl. At the bottom of each panel, the binding isotherm has been created by plotting the heat peak areas against the molar ratio of GA3 or ZEA added to the protein present in the cell. The line represents the best fit of a model with one independent binding site (*a*, *b*) or two sequential binding sites (*c*, *d*). One of three experiments is shown in each panel.

3.3. Thermodynamic characterization of PhBP–GA3 and PhBP–ZEA interactions

Table 3 presents the results of ITC titrations of VrPhBP and MtPhBP with GA3 and ZEA conducted at two pH conditions: 7.4 and 5.5. The assays revealed pH dependence of the binding of these two phytohormones, as well as confirming the specificity of the proteins towards GA3 binding and the nonspecific character of ZEA binding. Binding stoichiometry (*N* ligand molecules per one protein molecule) can be determined from titration curves that have sigmoidal shape, and this is the case for titrations of MtPhBP and VrPhBP with GA3 at pH 5.5 (Fig. 6) and for VrPhBP also at pH 7.4. For the PhBP–GA3 complexes, *N* can be (slightly) rounded down to 1, which agrees with the stoichiometry observed in the crystal structures. The small discrepancies (1.14 for MtPhBP and 1.09 for VrPhBP) can be attributed to the presence of a small amount of inactive protein molecules that for one reason or another (*e.g.* misfolding, denaturation or precipitation) lost their binding capability.

MtPhBP binds GA3 strongly at pH 5.5, with a dissociation constant K_d of 13.4 $\pm$ 0.5 µ*M*. No significant heat change was

observed during the titration of MtPhBP with GA3 at pH 7.4. The very small change in enthalpy ($\Delta H < 800$ cal mol^{-1}) during titration of MtPhBP with ZEA at pH 5.5 and 7.4 makes these measurements very unreliable and suggests a nonspecific interaction. All of these observations strongly suggest that MtPhBP is a very specific GA3 binder but only under slightly acidic conditions.

In the case of the VrPhBP protein, as previously reported by Pasternak *et al.* (2006), titration with ZEA yields hyperbolic curves despite the use of a high protein concentration (~100 μ*M*) in the sample cell (Figs. 6*c* and 6*d*). Our results (Table 3) are in very good agreement with the values reported for the VrPhBP–ZEA interaction (K_d = 106 ± 12 μ*M* at pH 6.5) by Pasternak *et al.* (2006). Both experiments are suggestive of a rather nonspecific character of ZEA binding. Because of the hyperbolic shape of the titration curves, the stoichiometry had to be fixed before fitting other model parameters. The stoichiometry of the VrPhBP–ZEA complex was assigned on the basis of the crystal structure (PDB entry 2flh), in which the protein:ligand ratio is 1:2 in three complex molecules and 1:1 in one complex molecule in the asymmetric unit. The binding model was selected as sequential binding sites as the second ligand molecule, bound near the entrance to the binding cavity, can only be docked after the deeper binding site has been filled. From this model, we can conclude that the binding of the first ZEA molecule is enthalpy-driven, whereas the binding of the second molecule leads to an entropy increase (Table 3). Fitting the data with a one set of binding sites model and a 1:1 stoichiometry yields a K_d value for ZEA binding that is only slightly lower than K_{d2} of the sequential binding sites model (66 ± 5 μ*M* at pH 5.5 and 60 ± 3 μ*M* at pH 7.4).

On the other hand, our results disagree with those reported by Zawadzki *et al.* (2010) at pH 7.2, where the K_d values for VrPhBP were estimated at 409 ± 32 and 383 ± 15 μ*M* for the interactions with ZEA and GA3, respectively. These authors, however, used a very large chromophore to label the ligands in their assays, which makes their results controversial, especially when the limited volume of the internal cavity is taken into account. Based on our results, VrPhBP shows a much higher affinity for GA3. Our K_d values of 23 ± 1 and 6.1 ± 0.2 μ*M* at pH 7.4 and 5.5, respectively, indicate strong interactions.

The ITC data clearly demonstrate that proteins from two different plants previously classified as Cytokinin-Specific Binding Proteins (CSBPs) are in fact relatively weak *trans*-zeatin binders and show a much higher affinity towards gibberellic acid. At acidic pH their affinity for GA3 is either (i) additionally increased, as is the case for VrPhBP, where the K_d decreases from ~23 to 6 μ*M* between pH 7.4 and 5.5, or (ii) switches from an absence of binding at pH 7.4 to enhanced binding at pH 5.5 (K_d = 13.4 μ*M*), as is the case for MtPhBP. Additionally, while GA3 binding by VrPhBP is exclusively enthalpy-driven, in the case of MtPhBP enthalpy and entropy drive the association process almost equally. This can be explained by the different chemical character of the residues surrounding the entrance to the internal cavity (Fig. 5). Specifically, charged residues in VrPhBP form hydrogen bonds to the ligand, contributing to an enthalpic effect, while hydrophobic interactions in the case of MtPhBP contribute to an entropy change.

The specificity of VrPhBPs towards gibberellic acid was additionally confirmed by a competitive binding (displacement) assay at pH 5.5, in which the protein was titrated with GA3 in the presence of *trans*-zeatin, added in advance at a concentration assuring saturation. The presence of a competing ligand (ZEA) changed the K_d of GA3 binding from 6 to 23 μ*M* and ΔH from −9039 to −4683 cal mol^{-1}. The titration curve remained sigmoidal. In addition, the binding parameters for ZEA in the first binding site of VrPhBP (K_{dZEA} and ΔH_{ZEA}) were tested using this displacement assay. From the apparent K_d (K_{dapp}) and ΔH (ΔH_{app}) one can determine the binding parameters of the low-affinity ligand (ZEA; *i.e.* the ligand being displaced) using (1) and (2) derived from Zhang & Zhang (1998),

$$K_{dZEA} = \frac{K_{dGA3}}{K_{dapp}} \times [\mathrm{ZEA}], \tag{1}$$

$$\Delta H_{ZEA} = (\Delta H_{GA3} - \Delta H_{app})\left(1 + \frac{K_{dZEA}}{[\mathrm{ZEA}]}\right), \tag{2}$$

where [ZEA] is the concentration of the low-affinity ligand (ZEA) and K_{dGA3} and ΔH_{GA3} are the dissociation constant and enthalpy change, respectively, obtained from titration with the high-affinity ligand only (GA3; Table 3). The calculated values of 113 μ*M* for K_{dZEA} and of −5489 cal mol^{-1} for ΔH_{ZEA} are in very good agreement with the values obtained in the direct titration experiment (Table 3).

It is very interesting to note that the dissociation constants for PhBP–GA3 interactions, 13.4 and 6.1 μ*M* at pH 5.5, are close to the value of 4 μ*M* reported for the gibberellin receptor GID1 (Ueguchi-Tanaka *et al.*, 2005). However, the above value of K_d for the GID1 receptor was determined at pH 7.6, which suggests that the PhBPs may be physiologically relevant gibberellin binders that are switched on by local pH decreases. While it is tempting to suggest that GA3 binding becomes relevant under acidic conditions, we note that there is no experimental evidence to suggest vacuolar or endosomal localization of the PhBP proteins.

3.4. PhBP proteins are adapted to bind gibberellic acid more potently than *trans*-zeatin

In the crystal structure of VrPhBP in complex with *trans*-zeatin (PDB entry 2flh), the phytohormone was bound in three different modes in the four copies of the protein molecule in the asymmetric unit (Pasternak *et al.*, 2006). Two instances of a head-to-head orientation of a tandem of ligand molecules (with adenine-ring stacking), in chains *A* and *D*, are almost identical. In chain *B* two ligands are bound in a head-to-tail fashion, whereas in chain *C* there is only one ZEA molecule inside the cavity. This binding diversity even within one crystal structure strongly suggests that *trans*-zeatin is not an optimal, and perhaps also not a biologically relevant, ligand for the protein. The picture with gibberellic acid binding,

where a single GA3 molecule is bound in exactly the same manner by two 'CSBP' orthologues, is certainly more convincing as biologically significant. Of course, this does not preclude the possibility that some other as yet unknown ligands (not only phytohormones) could also be binding partners of the PhBP proteins, especially in view of the large diversity of plant metabolites and signalling molecules and the documented ability of PR-10 proteins to bind different ligands (Fernandes *et al.*, 2013). However, at the present moment GA3 appears to be the best ligand for the PhBP subfamily.

The conformation of the VrPhBP protein is practically insensitive to the binding of either of the phytohormones, GA3 or ZEA. This is best illustrated by the small r.m.s.d. values on comparing the C^{α} atoms of the VrPhBP–GA3 complex with those of the VrPhBP–ZEA complexes, which were calculated in *UCSF Chimera* (Pettersen *et al.*, 2004) as 0.55 Å (for chains *C* and *D* of PDB entry 2flh) or 0.64 Å (chains *A* and *B*). The volume of the internal cavity is also unchanged and is calculated using *SURFNET* (Laskowski, 1995) as 915–950 $Å^3$. Since there is no crystal structure of a PhBP protein without a ligand, it is not possible to tell how much conformational change is needed for the binding of a given phytohormone. However, from the analysis of similar situations with other PR-10 proteins (Fernandes *et al.*, 2008; Sliwiak *et al.*, 2014) one can quite safely assume that the structural adjustment of the PhBP proteins is also minimal.

Our results have another important implication. For a number of years it has been postulated that PR-10 proteins show higher intraspecific than interspecific conservation (Wen *et al.*, 1997; Finkler *et al.*, 2005; Schenk *et al.*, 2009; Lebel *et al.*, 2010), and this assumption has made PR-10 proteins very good phylogenetic markers. Our work shows that the PhBP subfamily may be an exception in this context and that two proteins from different organisms can actually have conserved function.

4. Conclusions and outlook

This paper describes the crystal structures of two proteins from a PR-10 subfamily, originally classified as Cytokinin-Specific Binding Proteins (CSBP), in complex with a completely different phytohormone, gibberellic acid (GA3). These proteins bind GA3 strongly and specifically with a 1:1 stoichiometry, and the binding mode of this phytohormone is conserved. The crystallographic observations are corroborated by calorimetric experiments showing that the dissociation constants of the GA3 complexes are in the low micromolar range at pH 5.5. From this experimental evidence, supplemented with the observation that binding of a cytokinin ligand (*trans*-zeatin) is nonspecific, much weaker or absent altogether, we propose a revision of the annotation of these proteins as phytohormone-binding proteins (PhBP) to reflect their more likely (and more general) biological function.

The complexes with gibberellic acid described in this paper do not explain the universal role of PR-10 proteins. Nevertheless, the presented results show the PhBP subfamily in the context of gibberellic acid binding, which has not been considered before. The PhBP proteins share a low level of sequence identity (∼20%) with classic PR-10 proteins and they appear to have evolved to bind gibberellic acid and perhaps other gibberellins as well. The PhBPs could have evolved from an unknown common ancestor from which the abscisic acid (ABA) receptors have also originated. The ABA receptors have the PR-10 fold (Nishimura *et al.*, 2009; Santiago *et al.*, 2009) despite only marginal sequence identity. The assumption of a common ancestor could explain why these evolutionarily very distant proteins have retained the same overall fold. Apparently, it is a perfect fold for binding small-molecule, largely hydrophobic ligands such as phytohormones.

Based on a *BLAST* search (Altschul *et al.*, 1997), the PhBP homologues are only present in legume plants. This observation, however, has not been explained from a functional point of view. The strikingly low expression levels of PhBPs might suggest their biological role in plant hormone signalling pathways, as phytohormones are also present at very low concentrations.

Financial support for this project was provided by the European Union within the European Regional Developmental Fund and by the Polish Ministry of Science and Higher Education (grant Nos. NN 301 003739 and NN 301 204233). The research leading to these results received funding from the European Community's Seventh Framework Programme (FP7/2007-2013) BioStruct-X under grant agreement No. 283570. We thank Alina Kasperska for excellent technical assistance with recombinant protein production and purification.

References

Adams, P. D. *et al.* (2010). *Acta Cryst.* D**66**, 213–221.
Afonine, P. V., Grosse-Kunstleve, R. W., Echols, N., Headd, J. J., Moriarty, N. W., Mustyakimov, M., Terwilliger, T. C., Urzhumtsev, A., Zwart, P. H. & Adams, P. D. (2012). *Acta Cryst.* D**68**, 352–367.
Allen, F. H. (2002). *Acta Cryst.* B**58**, 380–388.
Altschul, S. F., Madden, T. L., Schäffer, A. A., Zhang, J., Zhang, Z., Miller, W. & Lipman, D. J. (1997). *Nucleic Acids Res.* **25**, 3389–3402.
Bradford, M. M. (1976). *Anal. Biochem.* **72**, 248–254.
Bujacz, G., Pasternak, O., Fujimoto, Y., Hashimoto, Y., Sikorski, M. M. & Jaskolski, M. (2003). *Acta Cryst.* D**59**, 522–525.
Chen, V. B., Arendall, W. B., Headd, J. J., Keedy, D. A., Immormino, R. M., Kapral, G. J., Murray, L. W., Richardson, J. S. & Richardson, D. C. (2010). *Acta Cryst.* D**66**, 12–21.
Chwastyk, M., Jaskolski, M. & Cieplak, M. (2014). *FEBS J.* **281**, 416–429.
Emsley, P., Lohkamp, B., Scott, W. G. & Cowtan, K. (2010). *Acta Cryst.* D**66**, 486–501.
Fernandes, H., Bujacz, A., Bujacz, G., Jelen, F., Jasinski, M., Kachlicki, P., Otlewski, J., Sikorski, M. M. & Jaskolski, M. (2009). *FEBS J.* **276**, 1596–1609.
Fernandes, H., Michalska, K., Sikorski, M. & Jaskolski, M. (2013). *FEBS J.* **280**, 1169–1199.
Fernandes, H., Pasternak, O., Bujacz, G., Bujacz, A., Sikorski, M. M. & Jaskolski, M. (2008). *J. Mol. Biol.* **378**, 1040–1051.
Finkler, C., Giacomet, C., Muschner, V. C., Salzano, F. M. & Freitas, L. B. (2005). *Genetica*, **124**, 117–125.
Fleet, C. M. & Sun, T.-P. (2005). *Curr. Opin. Plant Biol.* **8**, 77–85.
Fujimoto, Y., Nagata, R., Fukasawa, H., Yano, K., Azuma, M., Iida, A., Sugimoto, S., Shudo, K. & Hashimoto, Y. (1998). *Eur. J. Biochem.* **258**, 794–802.

Kabsch, W. (2010). *Acta Cryst.* D**66**, 125–132.
Kabsch, W. & Sander, C. (1983). *Biopolymers*, **22**, 2577–2637.
Kofler, S., Asam, C., Eckhard, U., Wallner, M., Ferreira, F. & Brandstetter, H. (2012). *J. Mol. Biol.* **422**, 109–123.
Krissinel, E. & Henrick, K. (2007). *J. Mol. Biol.* **372**, 774–797.
Kutschabsky, L. & Gunter, A. (1983). *J. Chem. Soc. Perkin Trans. 1*, pp. 1653–1655.
Langer, G., Cohen, S. X., Lamzin, V. S. & Perrakis, A. (2008). *Nature Protoc.* **3**, 1171–1179.
Larkin, M. A., Blackshields, G., Brown, N. P., Chenna, R., McGettigan, P. A., McWilliam, H., Valentin, F., Wallace, I. M., Wilm, A., Lopez, R., Thompson, J. D., Gibson, T. J. & Higgins, D. G. (2007). *Bioinformatics*, **23**, 2947–2948.
Laskowski, R. A. (1995). *J. Mol. Graph.* **13**, 323–330.
Lebel, S., Schellenbaum, P., Walter, B. & Maillot, P. (2010). *BMC Plant Biol.* **10**, 184.
Loon, L. C. van, Rep, M. & Pieterse, C. M. (2006). *Annu. Rev. Phytopathol.* **44**, 135–162.
Matthews, B. W. (1968). *J. Mol. Biol.* **33**, 491–497.
McCoy, A. J., Grosse-Kunstleve, R. W., Adams, P. D., Winn, M. D., Storoni, L. C. & Read, R. J. (2007). *J. Appl. Cryst.* **40**, 658–674.
Moriarty, N. W., Grosse-Kunstleve, R. W. & Adams, P. D. (2009). *Acta Cryst.* D**65**, 1074–1080.
Murase, K., Hirano, Y., Sun, T.-P. & Hakoshima, T. (2008). *Nature (London)*, **456**, 459–463.
Nishimura, N., Hitomi, K., Arvai, A. S., Rambo, R. P., Hitomi, C., Cutler, S. R., Schroeder, J. I. & Getzoff, E. D. (2009). *Science*, **326**, 1373–1379.
Pasternak, O., Bujacz, G. D., Fujimoto, Y., Hashimoto, Y., Jelen, F., Otlewski, J., Sikorski, M. M. & Jaskolski, M. (2006). *Plant Cell*, **18**, 2622–2634.
Peng, J., Richards, D. E., Hartley, N. M., Murphy, G. P., Devos, K. M., Flintham, J. E., Beales, J., Fish, L. J., Worland, A. J., Pelica, F., Sudhakar, D., Christou, P., Snape, J. W., Gale, M. D. & Harberd, N. P. (1999). *Nature (London)*, **400**, 256–261.
Pettersen, E. F., Goddard, T. D., Huang, C. C., Couch, G. S., Greenblatt, D. M., Meng, E. C. & Ferrin, T. E. (2004). *J. Comput. Chem.* **25**, 1605–1612.
Ruszkowski, M., Szpotkowski, K., Sikorski, M. & Jaskolski, M. (2013). *Acta Cryst.* D**69**, 2365–2380.
Santiago, J., Dupeux, F., Round, A., Antoni, R., Park, S.-Y., Jamin, M., Cutler, S. R., Rodriguez, P. L. & Márquez, J. A. (2009). *Nature (London)*, **462**, 665–668.
Santner, A., Calderon-Villalobos, L. I. & Estelle, M. (2009). *Nature Chem. Biol.* **5**, 301–307.
Schenk, M. F., Cordewener, J. H., America, A. H., Van't Westende, W. P., Smulders, M. J. & Gilissen, L. J. (2009). *BMC Plant Biol.* **9**, 24.
Schwechheimer, C. (2008). *Curr. Opin. Plant Biol.* **11**, 9–15.
Schwechheimer, C. & Willige, B. C. (2009). *Curr. Opin. Plant Biol.* **12**, 57–62.
Sliwiak, J., Jaskolski, M., Dauter, Z., McCoy, A. J. & Read, R. J. (2014). *Acta Cryst.* D**70**, 471–480.
Tomlin, C. D. S. (1997). Editor. *The Pesticide Manual: A World Compendium*, 11th ed., p. 639. Alton: BCPC.
Ueguchi-Tanaka, M., Ashikari, M., Nakajima, M., Itoh, H., Katoh, E., Kobayashi, M., Chow, T.-Y., Hsing, Y.-I., Kitano, H., Yamaguchi, I. & Matsuoka, M. (2005). *Nature (London)*, **437**, 693–698.
Wen, J., Vanek-Krebitz, M., Hoffmann-Sommergruber, K., Scheiner, O. & Breiteneder, H. (1997). *Mol. Phylogen. Evol.* **8**, 317–333.
Yabuta, T. & Sumitki, Y. (1938). *J. Agric. Chem. Soc. Jpn*, **14**, 1526.
Yamaguchi, S. (2008). *Annu. Rev. Plant Biol.* **59**, 225–251.
Zawadzki, P., Slósarek, G., Boryski, J. & Wojtaszek, P. (2010). *Biol. Chem.* **391**, 43–53.
Zhang, Y.-L. & Zhang, Z.-Y. (1998). *Anal. Biochem.* **261**, 139–148.